

Article

Evaluating a Nickel–Metal Hydride (NiMH) Battery Regeneration Patent Based on a Non-Intrusive and Unsupervised Prototype

Rafael Martínez-Sánchez, Angel Molina-García *, Antonio Mateo-Aroca  and Alfonso P. Ramallo-González

Department of Automatics, Electrical Engineering and Electronic Technology, Universidad Politecnica de Cartagena, 30202 Cartagena, Spain; rafael.martinez@edu.upct.es (R.M.-S.); antonio.mateo@upct.es (A.M.-A.); alfon sop.ramallo@upct.es (A.P.R.-G.)

* Correspondence: angel.molina@upct.es

Abstract: In the ongoing shift toward electric vehicles (EVs) primarily utilizing lithium-ion battery technology, a significant population of hybrid electric vehicles (HEVs) remains operational, which are reliant on established NiMH battery systems. Over the last twenty years, these HEVs have generated a substantial number of NiMH batteries that are either inoperable, experiencing performance degradation, or approaching the end of their service life. This situation results in a twofold challenge: (i) a growing volume of environmentally hazardous waste due to the difficulty of NiMH battery reclamation and (ii) escalating maintenance costs for HEV owners necessitated by replacement battery purchases. To overcome this scenario, patent WO2015092107A1, published in 2015, proposed a ‘Method for regenerating NiMH batteries.’ This method claimed the ability to restore NiMH batteries to their original functionality based on a non-intrusive approach. However, a comprehensive review of the relevant scientific literature fails to identify any empirical evidence supporting the efficacy of this regeneration technique. Within this context, this study provides a detailed analysis and evaluation of the regeneration process based on an unsupervised and non-intrusive prototype. The proposed prototype can be used not only to implement and evaluate the previous patent, but also to test any other process or methodology based on controlled charging/discharging periods under certain current conditions. NiMH battery cells from a Toyota Prius were included in this work as a real case study. The experimental results from this prototype demonstrate the reduced potential for battery regeneration using the proposed method. Future contributions should offer a promising solution for mitigating the challenges associated with NiMH battery disposal, maintenance within the HEV domain, and other second-life alternative options.

Keywords: battery regeneration; battery second life; circular economy



Citation: Martínez-Sánchez, R.; Molina-García, A.; Mateo-Aroca, A.; Ramallo-González, A.P. Evaluating a Nickel–Metal Hydride (NiMH) Battery Regeneration Patent Based on a Non-Intrusive and Unsupervised Prototype. *Batteries* **2024**, *10*, 402. <https://doi.org/10.3390/batteries10110402>

Received: 11 October 2024

Revised: 2 November 2024

Accepted: 8 November 2024

Published: 14 November 2024



Copyright: © 2024 by the authors. Licensee MDPI, Basel, Switzerland. This article is an open access article distributed under the terms and conditions of the Creative Commons Attribution (CC BY) license (<https://creativecommons.org/licenses/by/4.0/>).

1. Introduction

Over the past few years, several authors have analyzed the development and future of electric mobility [1–3]. The International Energy Agency (IEA), in its 2022 global electric vehicle (EV) outlook report, analyzed recent developments in electric mobility, including an analysis of the battery supply chain for electric vehicles. Their results indicated that sales of electric vehicles were growing at an exponential rate—for example, in 2021, this number was doubled when compared with the previous year—with the main drawback for electric vehicle sales being the price of materials for manufacturing batteries. The authors of [4] pointed out that around 230 million EVs will circulate in 2030, and their battery needs can be reduced through reuse, recycling, circular economy, and technological improvements. A decrease in the price of batteries by 2050 was predicted in [5], but the obstacle of the increasing material prices due to scarcity still exists, as affirmed in [6]. With this growth scenario for EV sales and the depletion of materials for manufacturing battery cells, the following problems can be identified: (i) The large number of batteries discarded

at the end of their useful life, which will probably grow exponentially with the sale of vehicles; (ii) a relevant waste problem caused by difficulties in recycling and reuse. Preeti and Sayali [7] examined the problem of recycling EV batteries and, according to them, 113 publications focused on recycling these batteries can be identified; and (iii) a lack of materials for manufacturing batteries.

Certain initiatives can extend the useful life of batteries through using them for services that are less-demanding than those of vehicles. For example, batteries that have lost part of their health can still store renewable energies, wherein the system is not affected by being stationary and does not require large spaces; alternatively, they can supply power during peak periods in power distribution systems [8]. Some studies have described the feasibility of giving a second life to lithium batteries from electric vehicles on a communication basis, concluding that using batteries this way reduces processing loads and environmental impacts. The authors of [9] analyzed how EV batteries at the end of their lives can serve as emergency storage in highly populated places, providing additional grid storage options during possible disasters. In this way, [10] estimated a 56% reduction in CO₂ emissions, compared with supplying that need with natural gas. Through a cascade life cycle analysis (LCA), the authors of [11] suggested a potential decrease in five main indicators—global warming potential, photochemical oxidation formation potential (POFP), particulate matter formation potential (PMFP), freshwater eutrophication potential (FEP), and fossil resource depletion potential (FDP)—based on the use of EV vehicle batteries in stationary applications after the end of their useful life. Through a life cycle analysis, the authors of [12] established that reductions in greenhouse gases (GHGs) in different types of lithium batteries varied between 2.76 and 4.55 kg CO₂/kg of battery, depending on the technology used for recycling, when comparing the use of recycled batteries to the production of new ones. Other contributions, such as [13], have analyzed the situation in China, comparing electric vehicle recycling through LCA. They concluded that, if batteries are recycled at the end of their lives, 34% GHG savings can be achieved compared with their original production processes. Indeed, notwithstanding the potential extension of battery lifespan, eventual disposal becomes inevitable, categorizing them as waste materials.

Numerous studies have described solutions to give batteries a second life [14–18]. They have concluded that reusing a battery is a viable option, as it can delay the need for recycling. Moreover, this also allows battery recycling companies to develop cost- and energy-efficient processes. The authors of [19] noted that the industry is currently not prepared for the mass dismantling of batteries that can generate recyclables and a true circular economy. Therefore, battery designs should be modified by considering dismantling and recycling with this criterion in mind. In most proposed solutions, the authors assert that it is imperative to extend the operational longevity of batteries, mitigating both economic and environmental ramifications. However, batteries will inevitably deplete and transition into waste materials, necessitating recycling measures. Technologies for recycling lead-acid-type batteries are well-known [20]; however, there is a lack of research on battery technologies for hybrid and electric vehicles. Recent contributions can be found in [21–24], mainly evaluating waste treatment processes. Innocenzi et al. [25] established a wide range of methods for recycling NiMH batteries, mainly through hydrometallurgical methods. Examples of this procedure can be found in other contributions [26–41]. However, mainly due to the specific requirements of the recycling process, these methods render the battery unusable for its original purpose by fully deconstructing it. This points to the relevance of proposing alternative approaches as a viable solution, such as battery regeneration. Instead of discarding batteries at the end of their operational lives, regeneration can potentially restore them to functional status. Additionally, this approach addresses the rising costs of raw materials by reducing the demand for new resources in battery production.

Battery regeneration has been used for a long time in lead acid battery technologies [42]. However, there have only been minor contributions regarding battery regeneration applied to other technologies. In [43], four methods for regenerating NiMH batteries were described,

including the patent-based method evaluated in the present paper [44]. In [45], the proposed method requires disassembling the battery structure to access the materials for regeneration. In [46], the method described lacked enough data for replication. In [47], an alternative method involved a charging technique extending the battery lifespan more effectively than regeneration. The fourth method, outlined in patent WO2015092107A1 [44], proposed regenerating batteries comprising multiple cells according to a specified cycle detailed in the patent. After the patent's publication, no further scientific literature has emerged either substantiating or refuting its efficacy. Table 1 summarizes these methods. Additionally, there is a lack of technical services specializing in battery regeneration based on this patent's method or any alternative approach. Under this framework, this study aims to practically and appropriately assess the regeneration process for NiMH batteries based on the method outlined in the patent described in [44], based on an unsupervised and non-intrusive prototype. The proposed prototype not only can implement and evaluate the previous patent, but also allows for testing of any other process or methodology based on controlled charging/discharging periods under certain constant current conditions. This evaluation was conducted through a prototype developed by the authors and a real-test experiment involving the practical application of the method to a Toyota Prius battery as a case study. The results provide valuable insights into its feasibility. The objectives of this work thus include an unsupervised prototype, implemented by the authors to verify the described patent's performance in terms of battery regeneration purposes, which can be extended and used in other battery regeneration solutions based on charging/discharging controlled cycles.

Table 1. NiMH regeneration methods.

Year of Publication	Published by	Method	Destructive Testing	Reference
2004	Paper	Current Pulses	No	[45]
2005	Paper	Ultrasound	No	[46]
2014	Patent	Current Pulses	No	[44]
2021	Patent	O ₂ addition	Yes	[48]

The rest of this study is structured as follows. Technical characteristics, electrical diagrams, and components are described in detail in Section 2, as well as the proposed method for evaluating the patent's performance. The case study results are provided in Section 3 and discussed in Section 4. Finally, conclusions are provided in Section 5.

2. Materials and Methods

2.1. General Description

In detail, patent WO2015092107A1 states that it is necessary to carry out a series of controlled discharges and charges at a constant current to regenerate a battery cell. With this aim, a standard battery charger or regenerator should be used. These solutions are commonly used to regenerate properly configured lead batteries. As noted in the patent, a Toyota Prius battery is preferable, as it includes 28 NiMH cells with a nominal voltage of 7.2 V and a capacity of 6.5 Ah. According to these controlled charging/discharging requirements, a prototype was proposed and implemented by the authors, which can simultaneously charge and discharge a group of 28 cells in a controlled manner at a constant intensity. The general operation scheme of the proposed methodology can be found in Figure 1.

Based on this operation scheme, Table 2 summarizes the main characteristics and ranges of the expected prototype. During the development phase of any process or system, it is crucial to create a prototype to assess its functionality and behavior. Even with a comprehensive plan or schematic, such as the one depicted in Figure 1, prototyping enables the practical validation and identification of potential issues that may not have been apparent during the planning stage. Through building a prototype, engineers and designers can test the feasibility of their ideas, identify design flaws or inefficiencies,

and gather valuable feedback from stakeholders and end users. The iterative process of prototyping and testing enables refinement and optimization, ultimately leading to more robust and effective final products or processes. Considering the operational scheme shown in Figure 1 and according to the specific characteristics of the prototype summarized in Table 2, the general operation of the prototype for both charging and discharging processes was developed (Figure 2). This approach not only supports thorough planning, but also simplifies accurately selecting equipment and seamlessly integrating electrical systems within the overall design process.

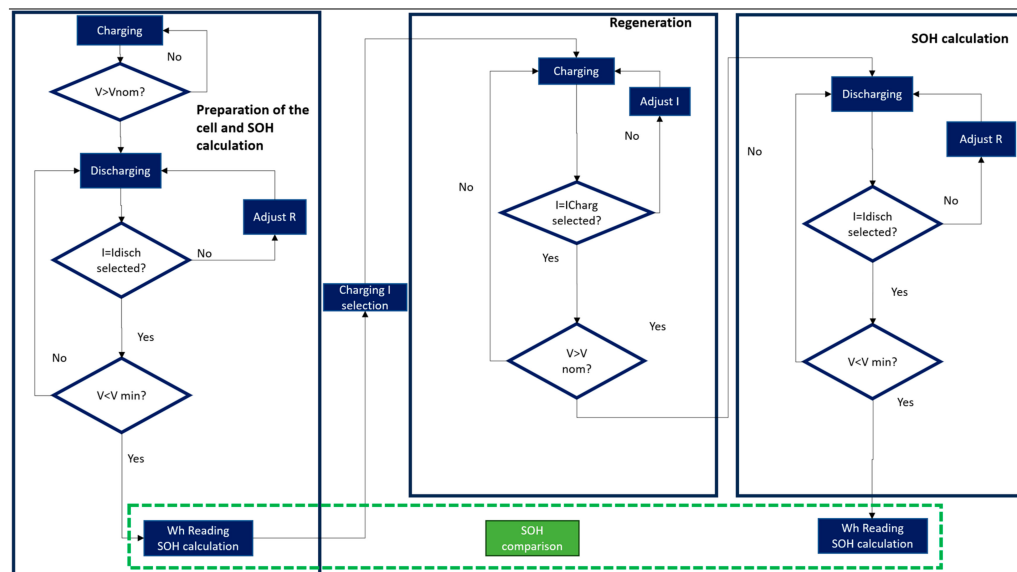


Figure 1. Operational scheme. General overview.

Table 2. Prototype characteristics.

Charging Values	Range
Voltage range	0–30 V
Current range	0–5 A
Discharging values	
Temperature range	–10–+60 °C
Voltage range	0–8.5 V
Current range	0–1 A
Operating and control values	
Capacity measurement range	0–99,999.9 Wh
Sample time	1 s
Minimum voltage power supply	7.5 V
Trigger (value for mode change)	0 V

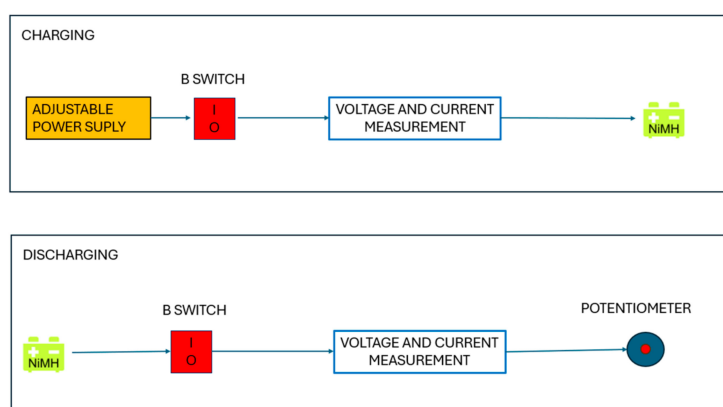


Figure 2. General operation of the prototype.

2.2. Prototype Description and Implementation

Based on the operational schemes depicted in Figure 2, Figure 3 summarizes the general electrical diagram of the prototype. This general scheme is subsequently characterized by both charging and discharging processes. With this aim, Figures 4 and 5 show the proposed electrical diagram for the corresponding charging and discharging processes for the proposed prototype. Based on these electrical diagrams, the authors implemented the prototype by considering the following components according to the number of cells to be regenerated. In this case, 28 adjustable current/voltage power supplies were proposed and implemented (Figure 6), through which the constant current at which each cell must be charged was selected. Each power source is then connected to a corresponding cell, charging in an individual process, consequently providing an independent process for each cell, as the patent suggests.

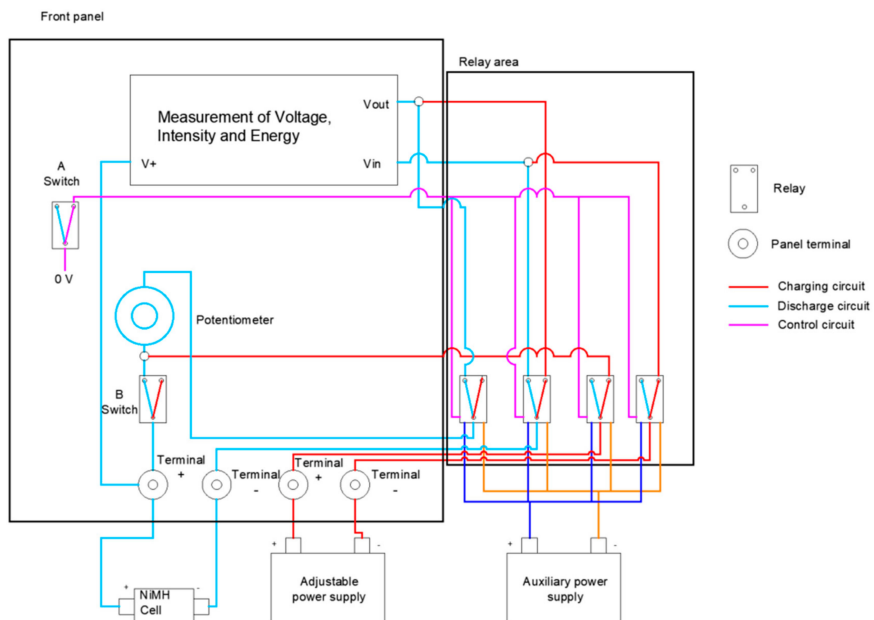


Figure 3. General electrical diagram of the prototype.

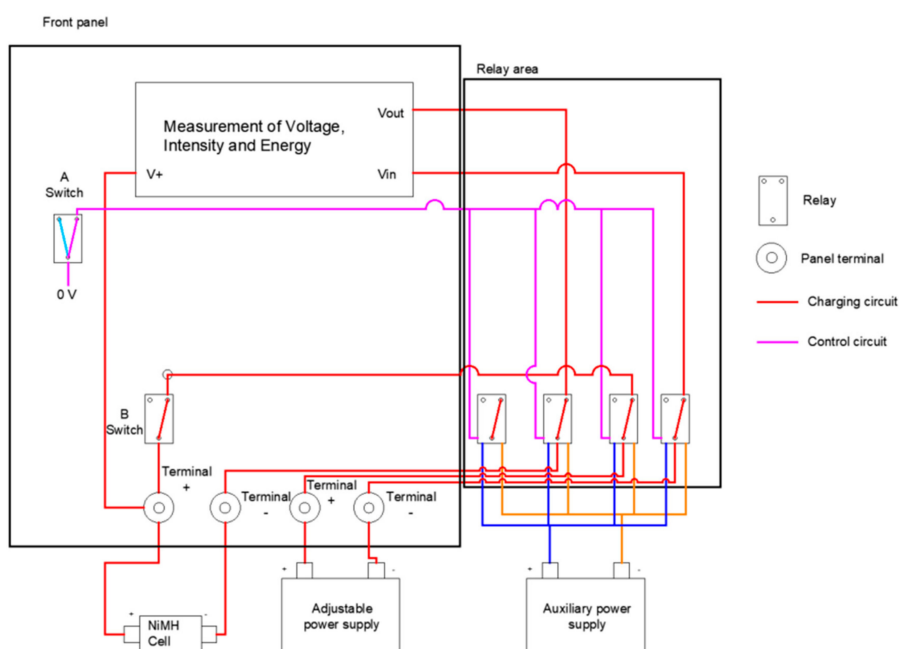


Figure 4. Electrical diagram of the prototype in charging mode.

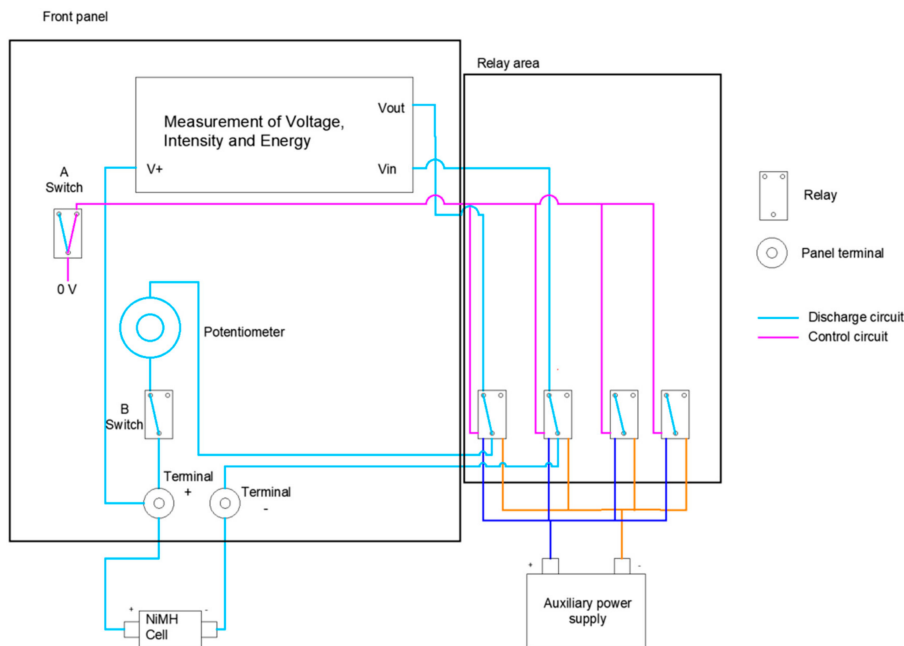


Figure 5. Electrical diagram of the prototype in discharging mode.



Figure 6. Power supplies for the cells and additional power supply for the process.

To discharge each cell in the battery, 28 potentiometers were selected, acting as the resistance through which the cells can be discharged, dissipating their energy in the form of heat (Figure 7). To discharge at a constant intensity, the current discharging values are readied on displays. The potentiometers are manually adjusted, thus varying their resistance. This is the resistance connected to each cell to be discharged under a constant discharge current value following the patent [44]. The potentiometers do not interact with any additional elements or alter the internal resistance of the cells; rather, they are adjustable resistance through which each cell discharges.



Figure 7. Potentiometer for the discharging process (TE Connectivity, Type 23 Series).

Figure 8 shows the monitoring system selected to track the voltage, current, and power flow—both charging and discharging processes—of individual cells within the regeneration battery process. This enables a comprehensive assessment of each cell's performance, allowing for accurate analysis and comparison throughout the regeneration process via 28 displays monitoring the previous parameters of each cell. To streamline the process and avoid the need to manually connect and disconnect each battery cell to various power supplies and potentiometers across multiple cycles, both the charging and discharging circuits were implemented in the device and separated via relays (Figure 9). Therefore, when one of the circuits is active, the other remains in open circuit conditions. Figure 8 shows that these circuits facilitate seamless switching between the two previous modes: charging and discharging. A single switch marked as 'A switch' in Figures 3–5 simultaneously provides the trigger signal to all relays and toggles all cells between the charging circuit, which connects the power sources to the cells; the discharging circuit connects the cells to the potentiometers acting as discharge resistors. Consequently, only the battery cells need to be connected to the prototype through their cell terminals, while all power sources are connected to the prototype through designated terminals. With the assistance of this switch, the entire battery can transition between charge and discharge modes in unison, enabling the simultaneous regeneration of all battery cells. Additionally, the prototype includes an individual switch for each battery cell (marked as 'B switch' in Figures 3–5), with 28 switches in total. Figure 10 shows an example of the selected switch. These switches isolate each cell, maintaining them in an open circuit state and thereby disconnecting them from the charging or discharging process. This functionality is crucial, as charging and discharging times may vary depending on the health status of each cell. Consequently, as each cell completes its independent cycle, it must be taken offline to await the completion of the processes by the remaining cells. Furthermore, each circuit is equipped with protection in the form of a fuse. Specifically, the discharge circuit is safeguarded by a 1 A fuse, while the charging circuit is protected by a 1.5 A fuse. Table 3 summarizes the selected component.



Figure 8. Display monitoring system (Caredy DT3010).



Figure 9. Example of the selected relay (Elego ASDIOFJ1).



Figure 10. Example of an A or B switch (RS PRO 1858229).

Table 3. Selected components for the prototype.

Component	Provided by	Model	Main Characteristics
Power supply for cells	Mlink (Beijing, China)	APS3005S	Adjustable power supply 0–30 V 0–5 A
Additional power supply	Mlink (Beijing, China)	APS6005D	Adjustable power supply 0–60 V 0–5 A
Potentiometer	TE Connectivity (Schaffhausen, Switzerland)	Type 23 Series	22 kΩ, one turn, panel mount
Display monitoring system	Caredy (Frederick, MD, USA)	DT3010	8–300 V DC, 0–100 A
Relay	Elego (Shenzhen, China)	ASDIOFJ1	
Switch	RS PRO (Fort Worth, TX, USA)	1858229	

An auxiliary power source has been integrated to supply power to the displays and relays, ensuring their seamless operation. To enhance user-friendliness and streamline operation, the components responsible for displaying data—as well as those facilitating battery and power source connections, potentiometer adjustment, and switch operation—were consolidated into a dedicated panel (Figures 11 and 12, respectively). This arrangement facilitates easier access and manipulation during usage. Additionally, to optimize organization and functionality, the panel hosting the relays responsible for circuit operation has been divided into a separate panel. This separation ensures clarity and efficiency in managing the regeneration process.

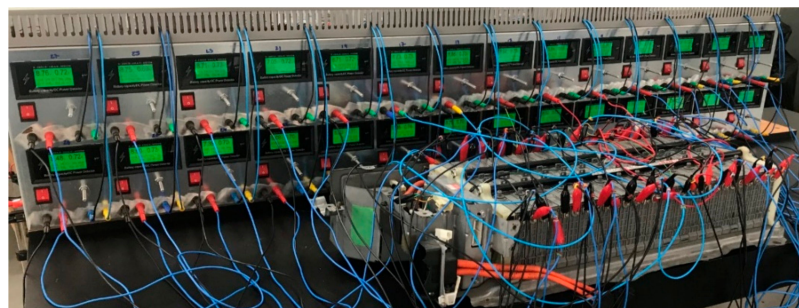


Figure 11. Frontal panel. General overview.



Figure 12. Rear panel with relays. Example.

The methodology involves initially preparing the battery by disassembling all protective components until achieving access to the terminals of each cell. Subsequently, the battery is connected to the prototype using terminals equipped with crocodile clips at the battery end and banana plugs at the prototype end. Following this setup, a series of sequential charging and discharging cycles are executed according to the method described in the patent.

3. Case Study

To assess the functionality outlined in the patent, cells were first selected for experimentation. To accomplish this, two Toyota Prius batteries comprising 56 cells were utilized, and the health status of each cell was meticulously evaluated. Various methods exist for evaluating cell health [49–52]. In this instance, the approach outlined in [53] was adopted, wherein the state of charge (SOC) is defined as the percentage of remaining capacity relative to the maximum available capacity of the battery [54]. This parameter can be expressed as

$$\text{SOC}(t) = \frac{\text{Cr}}{\text{Cm}} \times 100\%, \quad (1)$$

where Cr represents the residual capacity available for powering electric devices, and Cm denotes the maximum storage capacity of the cell, determined by its electrochemical characteristics. As per manufacturer specifications, each cell considered in this study has a capacity of $\text{Cm} = 46.42 \text{ Wh}$. To ascertain Cr, a series of charging cycles were conducted on each cell, reaching various charge levels, followed by discharging cycles to evaluate the amount of Wh discharged.

In the literature, various methodologies have been established to determine the SOC of battery cells [55,56]. However, in this specific investigation, charging and discharging procedures were conducted without adhering to any methods outlined in the scientific literature, in order to replicate the conditions stipulated in the patent. Initially, each cell was individually charged at a rate of 0.5 A until reaching a voltage of 8 V , considering the nominal voltage of the cells to be 7.2 V . Subsequently, each cell was discharged at a rate of 0.5 A until reaching a minimum voltage of 2 V . The discharge of any cell did not exceed 9 Wh in any instance, indicating a maximum state of health (SOH) of 19.39% . The SOH value was calculated as a comparison between the value of energy discharged in Wh provided by the device depicted in Figure 8 and the nominal value of energy capable of discharging the cell provided by the manufacturer, established at 46.42 Wh . This method is widely accepted, as indicated in [57], where $\text{SOH}(t)$ is defined as the nominal capacity at a certain time instant divided by the initial capacity (%). This method was also described and accepted in [58] as a suitable approach to estimate the SOH. Subsequently, a series of charging cycles was conducted with the same current as before while controlling the amount of energy charged. Following this, the cells were discharged, with the discharged energy measured to determine the Cc/Cm ratio, where Cc represents the charged energy. Concurrently, the SOH of each cell was calculated. The findings revealed that increasing the charged energy up to 15 Wh did not proportionally increase the amount of energy discharged, with some cells discharging up to 10.64 Wh , equivalent to a maximum SOH of 22.92% and a mean of 18.22% . Based on the SOH assessment of the battery, it can be inferred that all cells are in a similar state and notably below the 20% SOH threshold, indicating the end of the battery's life [59].

After assessing the battery condition, 21 cells were identified and selected based on their highest SOH value, or if they were deemed to be in suitable operational condition. Notably, some cells exhibited sulfated terminals yet were deemed viable for operation after following the instructions outlined in the patent [44]. Subsequently, each selected cell underwent a charging process at a constant rate of 0.5 A , followed by a discharge phase conducted in two stages. Initially, a rapid discharge was executed at 6.5 A until reaching a voltage of 5.4 V , according to the instructions outlined in the patent [44]. This was succeeded by a continuous discharge at a rate of 0.6 A until reaching a cut-off voltage of 2.4 V , as specified by the patent procedure. Throughout this procedure, the energies

charged and discharged were meticulously measured to ascertain the relationship between the two and to determine the SOH of each cell.

According to the patent, the regeneration process entails an anticipated enhancement in both charge and discharge capacity, as well as an improvement in cell SOH. Nevertheless, to ascertain the efficacy of the regeneration process, it was iteratively repeated up to nine times. The number of iterations was selected using the following equation [60]:

$$n = \left(\frac{Z_{\alpha/2} + Z_{\beta}}{\frac{\Delta}{\sigma}} \right)^2, \quad (2)$$

where N is the number of repetitions; $Z_{\alpha/2}$ is the Z-value corresponding to the desired confidence level (for 95%, the Z-value is 1.96); Z_{β} is the Z-value corresponding to the desired statistical power (for 80%, the value is 0.84); Δ is the effect size determined as a 25-point improvement in the SOH; and σ is the standard deviation of the process, chosen at 60 points, being the difference between the maximum and minimum charge level of each cell. Under these assumptions, the number of iterations necessary to observe the expected changes was eight, with nine iterations finally selected to be suitable for this study.

To correctly fulfill the patent, a predetermined cooling period was applied between each iteration. This cooling interval ensures that the cells present a sufficient steady-state temperature, preventing premature degradation and ensuring the integrity of the collected data. This iterative approach detects any trends indicating improved cell characteristics, gauging the success of the regeneration process, even if complete regeneration is not achieved in the initial cycle.

4. Results

The outcomes of the regeneration process are summarized in the subsequent graphs. Figure 13 illustrates the energy-charging process of the cells based on nine iterations of the regeneration process. In this way, the results obtained after the charging and discharging cycles are reported for each of the 28 cells, detailing the levels of stored energy achieved (kWh). Following these results and after nine iterations, no significant regeneration could be observed; all cells maintained charge levels between 14 and 16 kWh. The repeated charging and discharging at constant intensity did not facilitate the regeneration effect described in the patent process. In addition, the discharged energy of all cells iteratively subjected to the procedure is depicted in Figure 14. Similar to the previous case, the discharged energy (kWh) for each cell is represented across the nine iterations, with each cell numbered along the X-axis. This layout enables a vertical comparison of discharge levels for each cell corresponding to the relevant iteration, as indicated by the legend on the right side of the graph. Discharge levels—and, consequently, the available energy within each cell—were maintained between 7 and 10 kWh. This range provides insufficient evidence to assert that the regeneration process is functioning effectively in these cells. Moreover, these results enable comparative analysis across multiple cells, offering insights into the collective efficacy of the regeneration process. While a discernible trend toward enhanced discharge capacity appears evident with each successive regeneration, the cell's discharge values persist notably at markedly low levels. Similar marginal improvement trends in discharge capacity can be observed across the cells over successive regeneration cycles, and it is evident that the overall discharge values remain persistently low. This collective observation underscores the challenge in achieving substantial enhancements in cell performance through regeneration, despite repeated iterations. Figure 15 presents the progression of the discharged energy and charged energy ratio (in pu) throughout each regeneration process for each cell. It provides a comprehensive overview of how the discharged energy compares with the energy charged during each iteration of the regeneration process. Notably, in instances where the regeneration process has been executed, a noteworthy trend toward unity is anticipated, signifying a consistent ratio between discharged and charged energy. The convergence toward a value close to unity suggests a potential stabilization or

normalization of the energy balance within the cells following regeneration. This trend underscores the objective of achieving equilibrium between the energy input during charging and the energy output during discharge, indicating optimized cell performance.

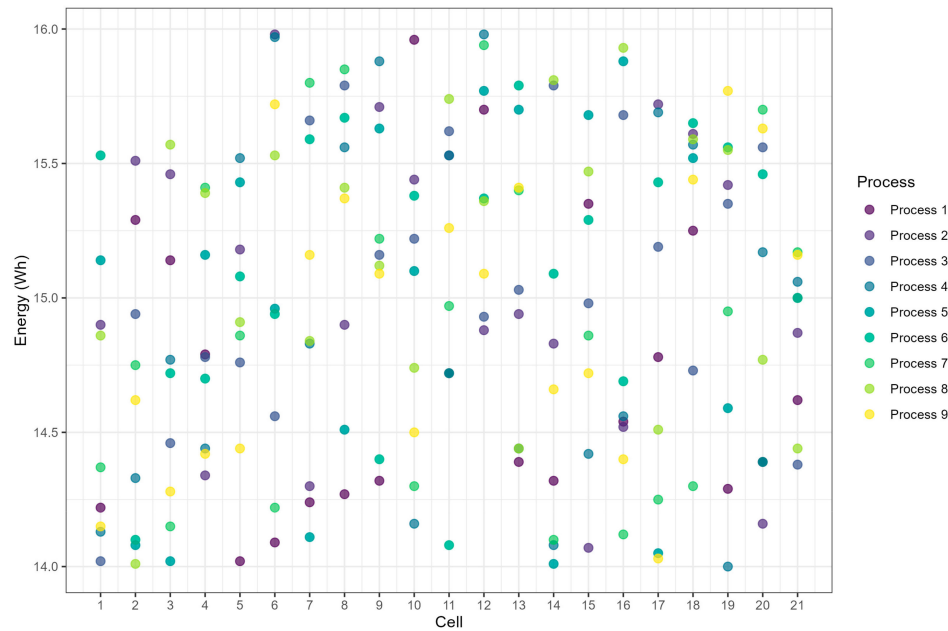


Figure 13. Energy charged in each cell. Data distribution for 9 process iterations.

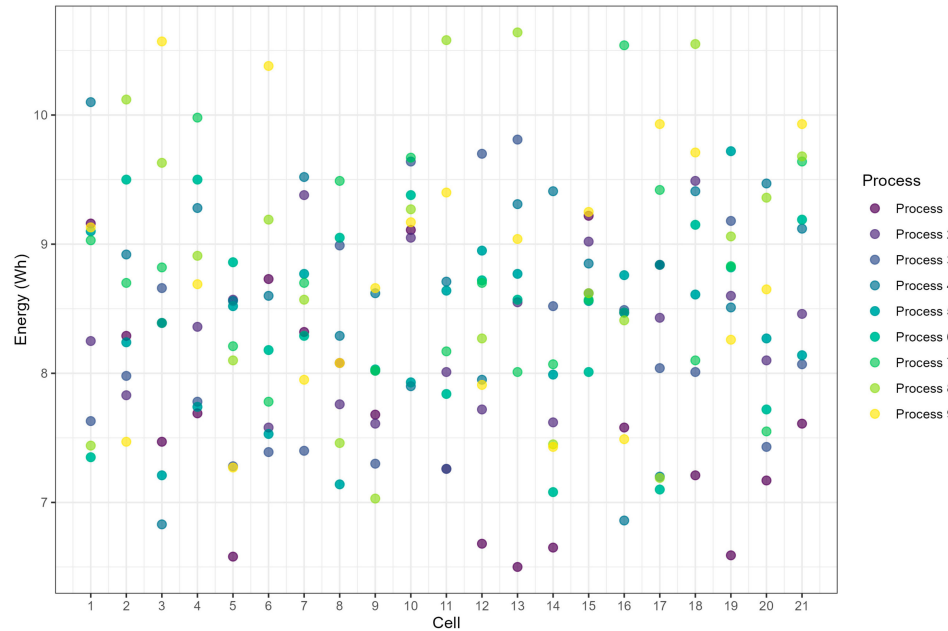


Figure 14. Energy discharged from each cell. Data distribution for 9 process iterations.

Figure 16 shows the dynamic evolution of the SOH across successive regeneration processes for each cell, providing a detailed examination of how this value evolves throughout the regeneration procedure. Generally, this analysis affirms that the regeneration process did not yield significant effects, as evidenced by the failure to achieve SOH values surpassing 23% across all cells. Additionally, a lack of discernible trends can be observed in most cells, suggesting that further iterations of the process may not yield substantial SOH improvements. While a discernible trend is observable in a few cells, its clarity is limited, and the overall efficacy of the regeneration process remains uncertain. Consequently, the data indicate that the current regeneration methodology may not be sufficiently robust

in restoring cells to optimal health levels. These findings underscore the need to either reassess and refine the regeneration approach to enhance its effectiveness and achieve meaningful improvements in cell performance or propose a second-life option (as discussed in Section 5).

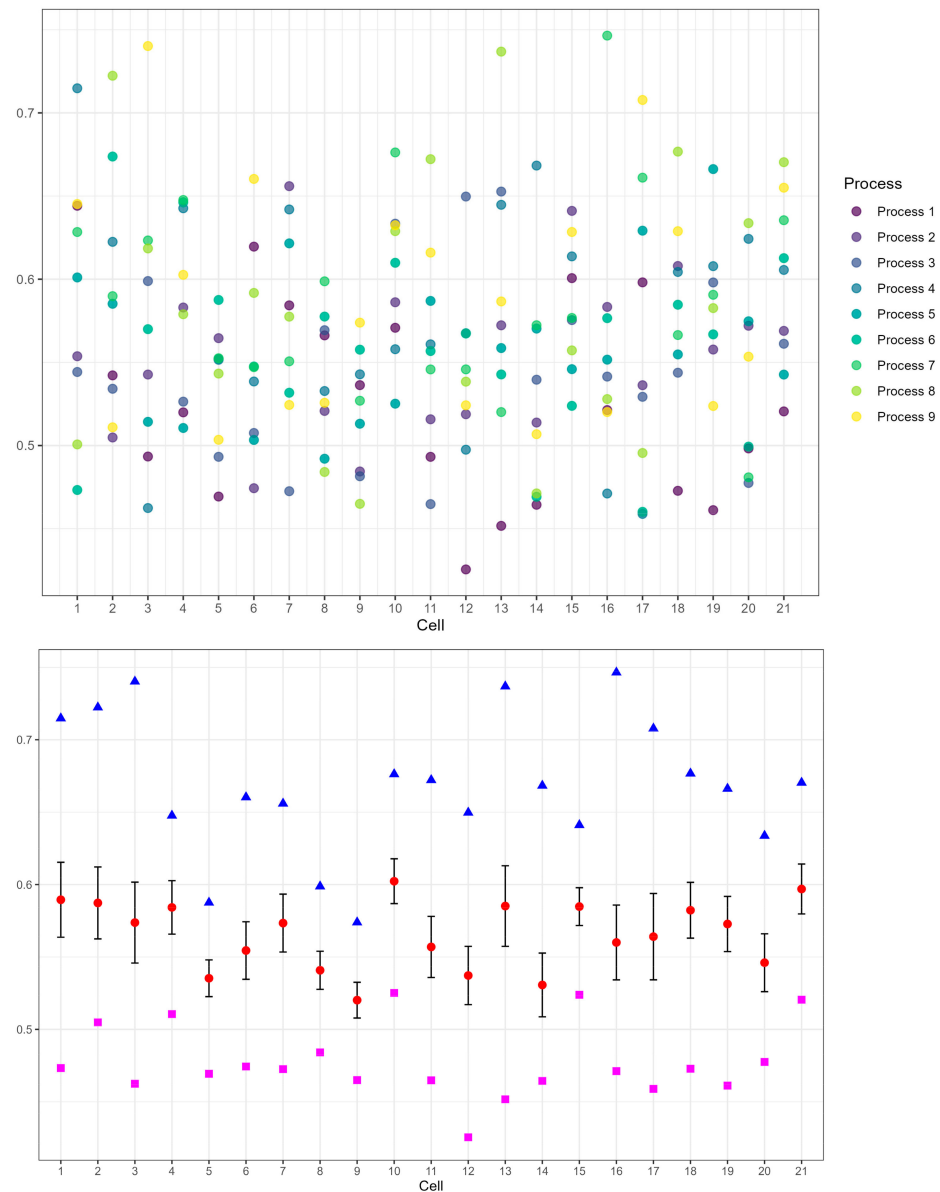


Figure 15. Ratio of energy discharged and charged for each cell (in pu). Data distribution for 9 process iterations and statistical analysis.

Additionally, further investigation into alternative regeneration techniques or supplementary interventions may be warranted to address the observed limitations and optimize battery cell rejuvenation. In cases where the regeneration process was effective, a conspicuous trend toward a value approaching 100% would be anticipated. This trajectory would signify a significant improvement in the health and functionality of the cells, approaching their optimal state. Conversely, a lack of discernible improvement or a trend toward values significantly below 100% would suggest the limited efficacy of the regeneration process in restoring the cells to their optimal health. Through monitoring SOH values over multiple cycles, valuable insights into the effectiveness and sustainability of the regeneration process can be gleaned, informing future strategies for battery maintenance, regeneration purposes, or second-life options.

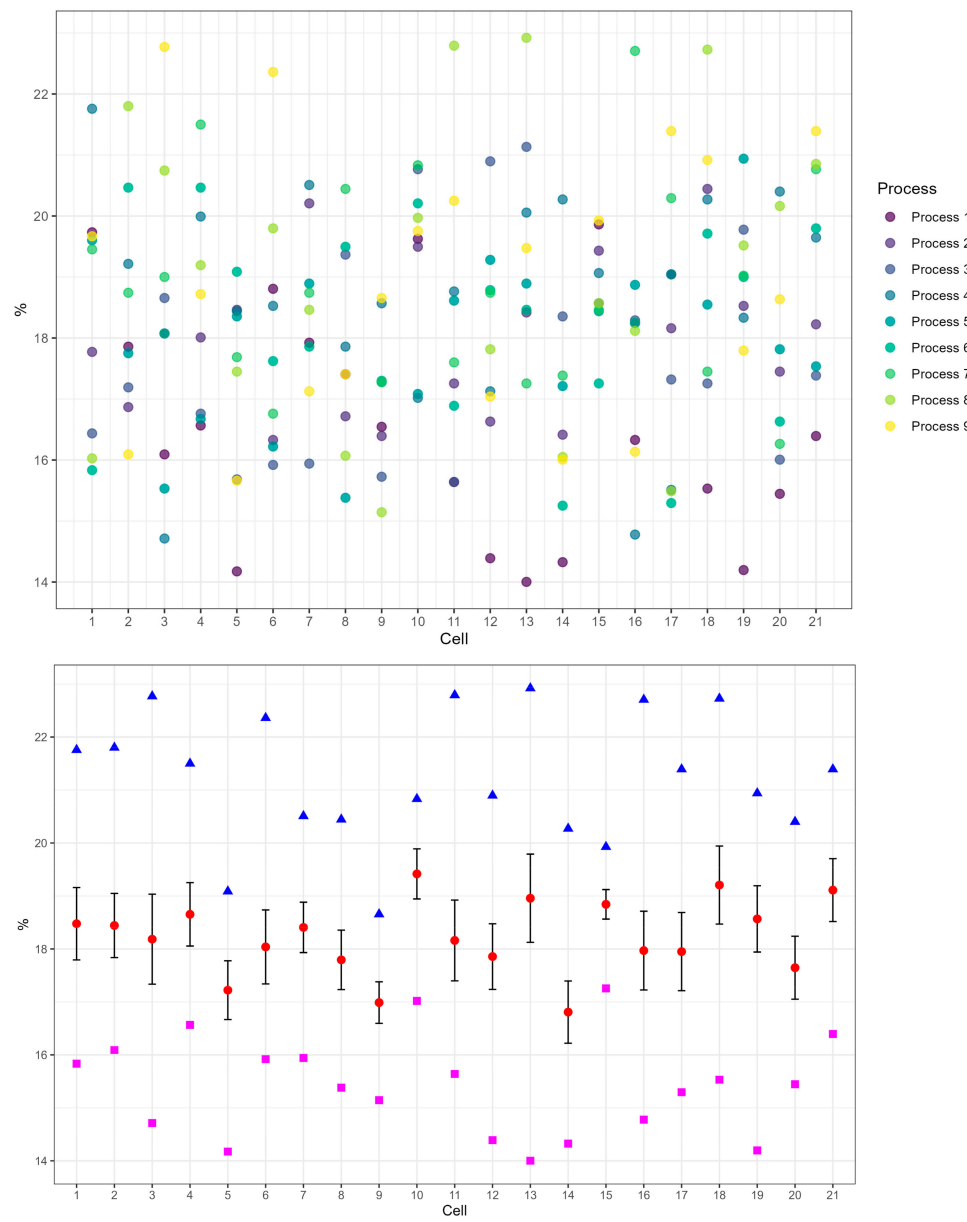


Figure 16. SOH in each cell for each process and statistical analysis.

Figures 17–19 provide a detailed evaluation of the SOH evolution for different cells that achieved comparatively high SOH values within the overall case study. These figures offer insights into the progression of SOH across the nine regeneration cycles calculated according to Equation (2). A significant improvement in SOH can be observed with each successive regeneration cycle, with relative enhancements ranging between 47% and 58% but with minor SOH enhancements, from 15% to 21% on average. This trend underscores the potential for substantial improvements in cell health through iterative regeneration processes, particularly in cells exhibiting initially high SOH values. The consistent upward trajectory in SOH values across multiple cycles suggests a promising avenue for significantly enhancing cell performance and longevity. However, further analysis is warranted to discern the underlying factors contributing to the observed improvements and to assess the sustainability of these gains over extended periods of operation. These findings underscore the importance of the ongoing monitoring and optimization of regeneration processes to maximize the efficacy of battery maintenance strategies.



Figure 17. SOH of cell 21 in each process.

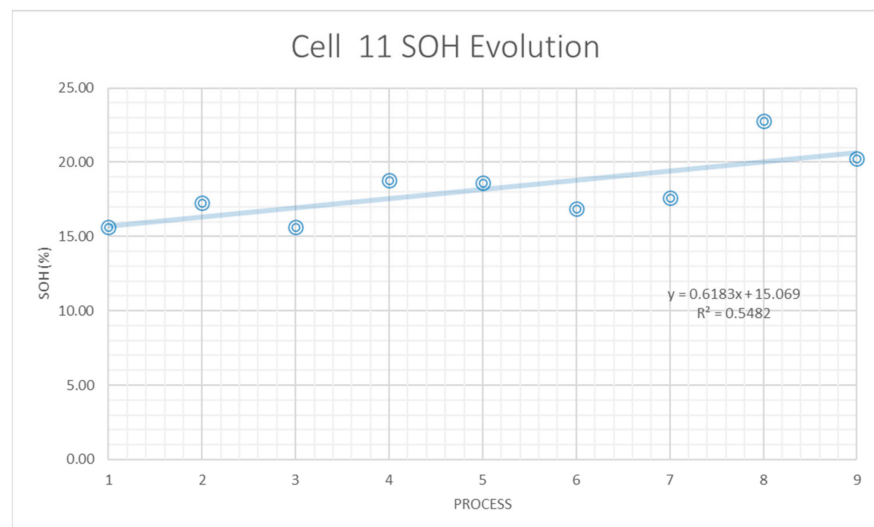


Figure 18. SOH of cell 11 in each process.

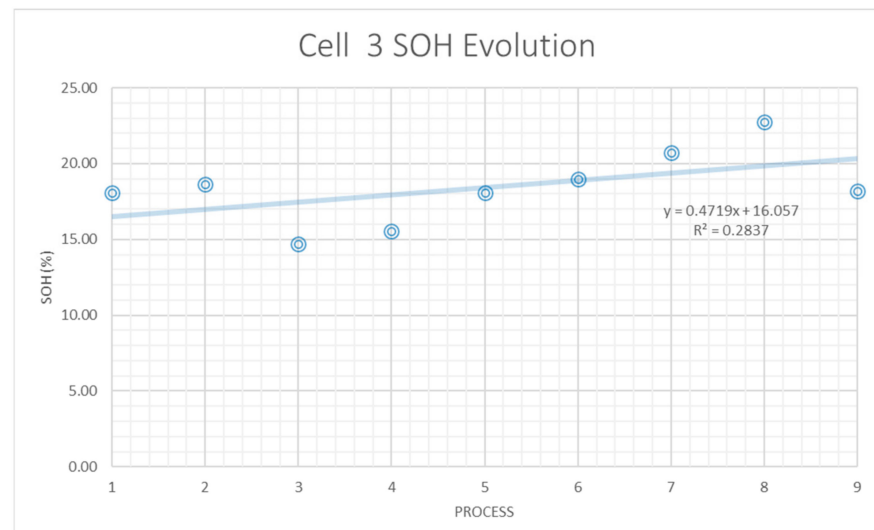


Figure 19. SOH of cell 3 in each process.

5. Discussion

To further advance this research, it is imperative to conduct similar tests using battery cells exhibiting a diverse range of SOH levels. The literature (such as [61]) suggests that vehicle batteries are commonly replaced when their SOH falls below 80%, with [62] proposing a replacement threshold within the 70–80% SOH range. Unfortunately, obtaining batteries with sufficiently high SOH levels for verification purposes proved challenging. The absence of suitable batteries precludes examining the regeneration efficacy at SOH levels of 70% or higher. Consequently, while this study concludes that the patent may not apply to cells beyond their useful lifespan, or those with severely diminished health, it remains inconclusive regarding the potential regeneration of cells with higher SOH values. A comprehensive follow-up study should involve a sizable sample of cells categorized based on their SOH levels, spanning 30% to 80% at 10% intervals, to ascertain the feasibility of regeneration across varying health states. Such verification would require developing an advanced prototype model capable of automation, particularly in streamlining processes such as automatically readjusting charging and discharging current conditions. An ideal prototype for this purpose could leverage advancements outlined in [63], which presents a battery characterization system incorporating internet of things (IoT) technology and low-cost hardware. Implementing such a prototype would enhance efficiency, reliability, and scalability, thereby facilitating rigorous and comprehensive experimentation to elucidate the potential and limitations of cell regeneration across a broad spectrum of SOH levels. This same study could be applied to lithium cells to check whether there is an effective change in their regeneration; according to [25], no contributions have been carried out on lithium cells following this method. Nevertheless, regarding SOH levels lower than 70%, battery second life is considered a promising approach for creating additional revenue streams that could lower initial EV costs for consumers. The prevailing view holds that batteries no longer suitable for EV applications may still perform adequately in less demanding settings, providing economic benefits in such roles [64]. In [65], the performance of NiMH batteries retired from EVs was compared with that of new lead–acid (PbA) batteries, considering four different stationary target applications in the U.S. market. The authors concluded that the considered second-life NiMH batteries performed at least as well as new PbA batteries. The EV batteries could even perform similarly to new PbA batteries over longer lifetimes in some scenarios. A few years later, Cready et al. [66] also presented a study of costs ranging from collection to reselling for refurbished second-life NiMH batteries in U.S. market conditions. In this study, transportation, testing, and EV battery refurbishment cost issues were considered. Although Cready et al. admitted uncertainties in their battery lifetime estimations, they claimed that the acquisition cost of the retired EV batteries and testing labors represented c.a. 70% of the total second-life battery costs. Wang et al. [67] analyzed the life cycle impacts of NiMH batteries, demonstrating that reuse or recycling significantly mitigates environmental burdens relative to disposal without recycling. Their findings show that reprocessing a waste NiMH battery—either through reuse or recycling rather than landfill disposal—can substantially diminish its environmental footprint. Specifically, the reuse and recycling scenario conserves approximately 83 kg of CO₂ emissions, 1.37 kg of resource depletion, 0.044 m³ of landfill space, and 1611 MJ of energy per battery, thus underscoring the environmental advantages of these strategies. More recently, Azizighalehsari et al. [68] affirmed that while second-life batteries offer distinct advantages, repurposing EV batteries for secondary applications introduces inherent technical and logistical complexities.

6. Conclusions

This study assessed the effectiveness of a patented method for regenerating NIMH cells. This evaluation was conducted using a prototype developed by the authors and through real-test experiments involving the practical application of the method to a deteriorated Toyota Prius battery. Following the proposed steps outlined in the patent, the cells were initially diagnosed to determine their state of health. Subsequently, the complete

regeneration process was applied to 21 selected cells. However, contrary to the expectations outlined in the patent, none of the cells showed signs of regeneration after the first application. In response to this unexpected outcome, the process was repeated nine consecutive times, adhering to time intervals specified in the patent. Despite these repeated attempts, none of the cells demonstrated any regeneration. In conclusion, our findings suggest that the regeneration process described in the patent is ineffective for cells with very low SOH values or those nearing the end of their lifespans. Further research and development efforts may be necessary to refine the regeneration process and improve its efficacy in such cases.

Author Contributions: Conceptualization, R.M.-S., A.M.-G., and A.P.R.-G.; methodology, R.M.-S. and A.M.-A.; formal analysis, R.M.-S. and A.P.R.-G.; resources, R.M.-S. and A.M.-A.; writing—original draft preparation, R.M.-S.; writing—review and editing, R.M.-S. and A.M.-A.; supervision, A.M.-G. All authors have read and agreed to the published version of the manuscript.

Funding: This research received no external funding.

Data Availability Statement: The data supporting the findings of this study are available from the corresponding author upon reasonable request.

Conflicts of Interest: The authors declare no conflicts of interest.

References

1. Kumar, R.R.; Alok, K. Adoption of electric vehicle: A literature review and prospects for sustainability. *J. Clean. Prod.* **2020**, *253*, 119911. [[CrossRef](#)]
2. Mounce, R.; Nelson, J.D. On the potential for one-way electric vehicle car-sharing in future mobility systems. *Transp. Res. Part. A Policy Pract.* **2019**, *120*, 17–30. [[CrossRef](#)]
3. Chian, T.Y.; Wei, W.L.J.; Ze, E.L.M.; Ren, L.Z.; Ping, Y.E.; Abu Bakar, N.Z.; Faizal, M.; Sivakumar, S. A Review on Recent Progress of Batteries for Electric Vehicles. *Int. J. Appl. Eng. Res.* **2019**, *14*, 4441–4461.
4. Nurdiawati, A.; Agrawal, T.K. Creating a circular EV battery value chain: End-of-life strategies and future perspective. *Resour. Conserv. Recycl.* **2022**, *185*, 106484. [[CrossRef](#)]
5. Mauler, L.; Duffner, F.; Zeier, W.G.; Leker, J. Battery cost forecasting: A review of methods and results with an outlook to 2050. *Energy Environ. Sci.* **2021**, *14*, 4712–4739. [[CrossRef](#)]
6. Turcheniuk, K.; Bondarev, D.; Amatucci, G.G.; Yushin, G. Battery materials for low-cost electric transportation. *Mater. Today* **2021**, *42*, 57–72. [[CrossRef](#)]
7. Preeti, M.; Sayali, A. Scientometric Analysis of Research on End-of-life Electronic Waste and Electric Vehicle Battery Waste. *J. Scientometr. Res.* **2021**, *10*, 37–46. [[CrossRef](#)]
8. Yang, J.; Gu, F.; Guo, J. Environmental feasibility of secondary use of electric vehicle lithium-ion batteries in communication base stations. *Resour. Conserv. Recycl.* **2020**, *156*, 104713. [[CrossRef](#)]
9. Moore, E.A.; Russell, J.D.; Babbitt, C.W.; Tomaszewski, B.; Clark, S.S. Spatial modeling of a second-use strategy for electric vehicle batteries to improve disaster resilience and circular economy. *Resour. Conserv. Recycl.* **2020**, *160*, 104889. [[CrossRef](#)]
10. Ahmadi, L.; Yip, A.; Fowler, M.; Young, S.B.; Fraser, R.A. Environmental feasibility of re-use of electric vehicle batteries. *Sustain. Energy Technol. Assess.* **2014**, *6*, 64–74. [[CrossRef](#)]
11. Ahmadi, L.; Young, S.B.; Fowler, M.; Fraser, R.A.; Achachlouei, M.A. A cascaded life cycle: Reuse of electric vehicle lithium-ion battery packs in energy storage systems. *Int. J. Life Cycle Assess.* **2017**, *22*, 111–124. [[CrossRef](#)]
12. Rosenberg, S.; Kurz, L.; Huster, S.; Wehrstein, S.; Kiemel, S.; Schultmann, F.; Reichert, F.; Wörner, R.; Glöser-Chahoud, S. Combining dynamic material flow analysis and life cycle assessment to evaluate environmental benefits of recycling—A case study for direct and hydrometallurgical closed-loop recycling of electric vehicle battery systems. *Resour. Conserv. Recycl.* **2023**, *198*, 107145. [[CrossRef](#)]
13. Hao, H.; Qiao, Q.; Liu, Z.; Zhao, F. Impact of recycling on energy consumption and greenhouse gas emissions from electric vehicle production: The China 2025 case. *Resour. Conserv. Recycl.* **2017**, *122*, 114–125. [[CrossRef](#)]
14. Hossain, E.; Murtaugh, D.; Mody, J.; Faruque, H.M.R.; Haque Sunny, M.d.S.; Mohammad, N. A Comprehensive Review on Second-Life Batteries: Current State, Manufacturing Considerations, Applications, Impacts, Barriers & Potential Solutions, Business Strategies, and Policies. *IEEE Access* **2019**, *7*, 73215–73252. [[CrossRef](#)]
15. Zhao, Y.; Pohl, O.; Bhatt, A.I.; Collis, G.E.; Mahon, P.J.; Rüther, T.; Hollenkamp, A.F. A Review on Battery Market Trends, Second-Life Reuse, and Recycling. *Sustain. Chem.* **2021**, *2*, 167–205. [[CrossRef](#)]
16. Deng, Y.; Zhang, Y.; Luo, F.; Mu, Y. Operational Planning of Centralized Charging Stations Utilizing Second-Life Battery Energy Storage Systems. *IEEE Trans. Sustain. Energy* **2021**, *12*, 387–399. [[CrossRef](#)]
17. Shahjalal, M.; Roy, P.K.; Shams, T.; Fly, A.; Chowdhury, J.I.; Ahmed, M.d.R.; Liu, K. A review on second-life of Li-ion batteries: Prospects, challenges, and issues. *Energy* **2022**, *241*, 122881. [[CrossRef](#)]
18. Kotak, Y.; Marchante Fernández, C.; Canals Casals, L.; Kotak, B.S.; Koch, D.; Geisbauer, C.; Trilla, L.; Gómez-Núñez, A.; Schweiger, H.-G. End of Electric Vehicle Batteries: Reuse vs. Recycle. *Energies* **2021**, *14*, 2217. [[CrossRef](#)]

19. Glöser-Chahoud, S.; Huster, S.; Rosenberg, S.; Baazouzi, S.; Kiemel, S.; Singh, S.; Schneider, C.; Weeber, M.; Miehe, R.; Schultmann, F. Industrial disassembling as a key enabler of circular economy solutions for obsolete electric vehicle battery systems. *Resour. Conserv. Recycl.* **2021**, *174*, 105735. [[CrossRef](#)]
20. Li, M.; Yang, J.; Liang, S.; Hou, H.; Hu, J.; Liu, B.; Kumar, R. Review on clean recovery of discarded/spent lead-acid battery and trends of recycled products. *J. Power Sources* **2019**, *436*, 226853. [[CrossRef](#)]
21. Yu, Y.; Chen, B.; Huang, K.; Wang, X.; Wang, D. Environmental Impact Assessment and End-of-Life Treatment Policy Analysis for Li-Ion Batteries and Ni-MH Batteries. *Int. J. Environ. Res. Public Health* **2014**, *11*, 3185–3198. [[CrossRef](#)] [[PubMed](#)]
22. Pindar, S.; Dhawan, N. Recycling of mixed discarded lithium-ion batteries via microwave processing route. *Sustain. Mater. Technol.* **2020**, *25*, e00157. [[CrossRef](#)]
23. Zeng, X.; Li, J.; Ren, Y. Prediction of various discarded lithium batteries in China. In Proceedings of the 2012 IEEE International Symposium on Sustainable Systems and Technology (ISSST), Boston, MA, USA, 16–18 May 2012; IEEE: Piscataway, NJ, USA, 2012; pp. 1–4. [[CrossRef](#)]
24. Jo, C.-H.; Myung, S.-T. Efficient recycling of valuable resources from discarded lithium-ion batteries. *J. Power Sources* **2019**, *426*, 259–265. [[CrossRef](#)]
25. Innocenzi, V.; Ippolito, N.M.; De Michelis, I.; Prisciandaro, M.; Medici, F.; Vegliò, F. A review of the processes and lab-scale techniques for the treatment of spent rechargeable NiMH batteries. *J. Power Sources* **2017**, *362*, 202–218. [[CrossRef](#)]
26. Zhang, P.; Yokoyama, T.; Itabashi, O.; Wakui, Y.; Suzuki, T.M.; Inoue, K. Hydrometallurgical process for recovery of metal values from spent nickel-metal hydride secondary batteries. *Hydrometallurgy* **1998**, *50*, 61–75. [[CrossRef](#)]
27. Zhang, P.; Yokoyama, T.; Itabashi, O.; Wakui, Y.; Suzuki, T.M.; Inoue, K. Recovery of metal values from spent nickel–metal hydride rechargeable batteries. *J. Power Sources* **1999**, *77*, 116–122. [[CrossRef](#)]
28. Pietrelli, L.; Bellomo, B.; Fontana, D.; Montereali, M.R. Rare earths recovery from NiMH spent batteries. *Hydrometallurgy* **2002**, *66*, 135–139. [[CrossRef](#)]
29. Rabah, M.A.; Farghaly, F.E.; Abd-El Motaleb, M.A. Recovery of nickel, cobalt and some salts from spent Ni-MH batteries. *Waste Manag.* **2008**, *28*, 1159–1167. [[CrossRef](#)]
30. Meshram, P.; Somani, H.; Pandey, B.D.; Mankhand, T.R.; Deveci, H.; Abhilash. Two stage leaching process for selective metal extraction from spent nickel metal hydride batteries. *J. Clean. Prod.* **2017**, *157*, 322–332. [[CrossRef](#)]
31. Santos, V.E.O.; Celante, V.G.; Lelis, M.F.F.; Freitas, M.B.J.G. Chemical and electrochemical recycling of the nickel, cobalt, zinc and manganese from the positives electrodes of spent Ni–MH batteries from mobile phones. *J. Power Sources* **2012**, *218*, 435–444. [[CrossRef](#)]
32. Nayil, A.A. Extraction and separation of Co(II) and Ni(II) from acidic sulfate solutions using Aliquat 336. *J. Hazard Mater.* **2010**, *173*, 223–230. [[CrossRef](#)] [[PubMed](#)]
33. Provazi, K.; Campos, B.A.; Espinosa, D.C.R.; Tenório, J.A.S. Metal separation from mixed types of batteries using selective precipitation and liquid–liquid extraction techniques. *Waste Manag.* **2011**, *31*, 59–64. [[CrossRef](#)] [[PubMed](#)]
34. Kanamori, T.; Matsuda, M.; Miyake, M. Recovery of rare metal compounds from nickel–metal hydride battery waste and their application to CH₄ dry reforming catalyst. *J. Hazard. Mater.* **2009**, *169*, 240–245. [[CrossRef](#)] [[PubMed](#)]
35. Innocenzi, V.; Vegliò, F. Recovery of rare earths and base metals from spent nickel–metal hydride batteries by sequential sulphuric acid leaching and selective precipitations. *J. Power Sources* **2012**, *211*, 184–191. [[CrossRef](#)]
36. Bertuol, D.A.; Amado, F.D.R.; Veit, H.; Ferreira, J.Z.; Bernardes, A.M. Recovery of Nickel and Cobalt from Spent NiMH Batteries by Electrowinning. *Chem. Eng. Technol.* **2012**, *35*, 2084–2092. [[CrossRef](#)]
37. Li, L.; Xu, S.; Ju, Z.; Wu, F. Recovery of Ni, Co and rare earths from spent Ni–metal hydride batteries and preparation of spherical Ni(OH)₂. *Hydrometallurgy* **2009**, *100*, 41–46. [[CrossRef](#)]
38. Rodrigues, L.E.O.C.; Mansur, M.B. Hydrometallurgical separation of rare earth elements, cobalt and nickel from spent nickel–metal–hydride batteries. *J. Power Sources* **2010**, *195*, 3735–3741. [[CrossRef](#)]
39. Gasser, M.S.; Aly, M.I. Separation and recovery of rare earth elements from spent nickel–metal–hydride batteries using synthetic adsorbent. *Int. J. Miner. Process.* **2013**, *121*, 31–38. [[CrossRef](#)]
40. Innocenzi, V.; Veglio, F. Separation of manganese, zinc and nickel from leaching solution of nickel–metal hydride spent batteries by solvent extraction. *Hydrometallurgy* **2012**, *129–130*, 50–58. [[CrossRef](#)]
41. Ahn, N.-K.; Shim, H.-W.; Kim, D.-W.; Swain, B. Valorization of waste NiMH battery through recovery of critical rare earth metal: A simple recycling process for the circular economy. *Waste Manag.* **2020**, *104*, 254–261. [[CrossRef](#)]
42. Sun, R.L.; Hu, P.Q.; Wang, R.; Qi, L.Y. A new method for charging and repairing Lead-acid batteries. *IOP Conf. Ser. Earth Environ. Sci.* **2020**, *461*, 12031. [[CrossRef](#)]
43. Martínez-Sánchez, R.; Molina-García, A.; Ramallo-González, A.P. Regeneration of Hybrid and Electric Vehicle Batteries: State-of-the-Art Review, Current Challenges, and Future Perspectives. *Batteries* **2024**, *10*, 101. [[CrossRef](#)]
44. Rodrigo Gómez Pérez, R.; Omaña Martin, A. Method to Regenerate Ni-MH Batteries. ES201331851A, 9 June 2016.
45. Zhang, J.; Yu, J.; Cha, C.; Yang, H. The effects of pulse charging on inner pressure and cycling characteristics of sealed Ni/MH batteries. *J. Power Sources* **2004**, *136*, 180–185. [[CrossRef](#)]
46. Li, L.; Wu, F.; Chen, R.; Gao, X.; Shan, Z. A new regeneration process for spent nickel/metal hydride batteries. *Trans. Nonferrous Metal. Soc. China* **2005**, *4*, 764–768.

47. Chen, P.; Yang, F.; Cao, Z.; Jhang, J.; Gao, H.; Yang, M.; Huang, K.D. Reviving Aged Lithium-Ion Batteries and Prolonging their Cycle Life by Sinusoidal Waveform Charging Strategy. *Batter. Supercaps* **2019**, *2*, 673–677. [[CrossRef](#)]
48. Shen, Y.; Starborg, S. Method for Reconditioning NiMH Battery Cells. US20230102119A1, 30 March 2023.
49. Blanke, H.; Bohlen, O.; Buller, S.; De Doncker, R.W.; Fricke, B.; Hammouche, A.; Linzen, D.; Thele, M.; Sauer, D.U. Impedance measurements on lead–acid batteries for state-of-charge, state-of-health and cranking capability prognosis in electric and hybrid electric vehicles. *J. Power Sources* **2005**, *144*, 418–425. [[CrossRef](#)]
50. Li, W.; Rentemeister, M.; Badeda, J.; Jöst, D.; Schulte, D.; Sauer, D.U. Digital twin for battery systems: Cloud battery management system with online state-of-charge and state-of-health estimation. *J. Energy Storage* **2020**, *30*, 101557. [[CrossRef](#)]
51. Kim, J.; Yu, J.; Kim, M.; Kim, K.; Han, S. Estimation of Li-ion Battery State of Health based on Multilayer Perceptron: As an EV Application. *IFAC-PapersOnLine* **2018**, *51*, 392–397. [[CrossRef](#)]
52. Galeotti, M.; Giannanco, C.; Cinà, L.; Cordiner, S.; Di Carlo, A. Synthetic methods for the evaluation of the State of Health (SOH) of nickel-metal hydride (NiMH) batteries. *Energy Convers. Manag.* **2015**, *92*, 1–9. [[CrossRef](#)]
53. Wang, Z.; Feng, G.; Zhen, D.; Gu, F.; Ball, A. A review on online state of charge and state of health estimation for lithium-ion batteries in electric vehicles. *Energy Rep.* **2021**, *7*, 5141–5161. [[CrossRef](#)]
54. Kim, I.-S. Nonlinear State of Charge Estimator for Hybrid Electric Vehicle Battery. *IEEE Trans. Power Electron.* **2008**, *23*, 2027–2034. [[CrossRef](#)]
55. Wu, G.; Lu, R.; Zhu, C.; Chan, C.C. State of charge Estimation for NiMH Battery based on electromotive force method. In Proceedings of the 2008 IEEE Vehicle Power and Propulsion Conference, Harbin, China, 3–5 September 2008; IEEE: Piscataway, NJ, USA, 2008; pp. 1–5. [[CrossRef](#)]
56. Bundy, K.; Karlsson, M.; Lindbergh, G.; Lundqvist, A. An electrochemical impedance spectroscopy method for prediction of the state of charge of a nickel-metal hydride battery at open circuit and during discharge. *J. Power Sources* **1998**, *72*, 118–125. [[CrossRef](#)]
57. Barré, A.; Deguilhem, B.; Grolleau, S.; Gérard, M.; Suard, F.; Riu, D. A review on lithium-ion battery ageing mechanisms and estimations for automotive applications. *J. Power Sources* **2013**, *241*, 680–689. [[CrossRef](#)]
58. Xing, Y.; Williard, N.; Tsui, K.-L.; Pecht, M. A comparative review of prognostics-based reliability methods for Lithium batteries. In Proceedings of the 2011 Prognostics and System Health Management Conference, Shenzhen, China, 24–25 May 2011; IEEE: Piscataway, NJ, USA, 2011; pp. 1–6. [[CrossRef](#)]
59. Hu, X.; Feng, F.; Liu, K.; Zhang, L.; Xie, J.; Liu, B. State estimation for advanced battery management: Key challenges and future trends. *Renew. Sustain. Energy Rev.* **2019**, *114*, 109334. [[CrossRef](#)]
60. Cohen, J. *Statistical Power Analysis for the Behavioral Sciences*; Routledge: London, UK, 2013. [[CrossRef](#)]
61. Zhu, J.; Mathews, I.; Ren, D.; Li, W.; Cogswell, D.; Xing, B.; Sedlatschek, T.; Kantareddy, S.N.R.; Yi, M.; Gao, T.; et al. End-of-life or second-life options for retired electric vehicle batteries. *Cell Rep. Phys. Sci.* **2021**, *2*, 100537. [[CrossRef](#)]
62. Maharan, S.; Jana, M.; Basu, S. Handling of the End of Life Electric Vehicle Batteries for Stationary Storage Applications. In Proceedings of the 2019 IEEE Transportation Electrification Conference (ITEC-India), Bengaluru, India, 17–19 December 2019; IEEE: Piscataway, NJ, USA, 2019; pp. 1–5. [[CrossRef](#)]
63. Martínez-Sánchez, R.; Molina-García, Á.; Ramallo-González, A.P.; Sánchez-Valverde, J.; Úbeda-Miñarro, B. A Low-Cost Hardware Architecture for EV Battery Cell Characterization Using an IoT-Based Platform. *Sensors* **2023**, *23*, 816. [[CrossRef](#)]
64. Martínez-Laserna, I.E.; Gandiaga, E.; Sarasketa-Zabala, J.; Badeda, D.-I.; Stroe, M.; Swierczynski, A. Goikoetxea, Battery second life: Hype, hope or reality? A critical review of the state of the art. *Renew. Sustain. Energy Rev.* **2018**, *93*, 701–718. [[CrossRef](#)]
65. Pinsky, N. *Electric Vehicle Battery 2nd Use Study*; Argonne National Laboratory: Argonne, IL, USA, 1998.
66. Cready, E.; Lippert, J.; Pihl, J.; Weinstock, I. *Technical and Economic Feasibility of Applying Used EV Batteries in Stationary Applications*; No. SAND2002-4084; Sandia National Lab. (SNL-NM): Albuquerque, NM, USA; Sandia National Lab. (SNL-CA): Livermore, CA, USA, 2003.
67. Wang, S.; Yu, J.; Okubo, K. Life cycle assessment on the reuse and recycling of the nickel-metal hydride battery: Fleet-based study on hybrid vehicle batteries from Japan. *J. Ind. Ecol.* **2021**, *25*, 1236–1249. [[CrossRef](#)]
68. Azizighalehsari, S.; Venugopal, P.; Pratap Singh, D.; Batista Soeiro, T.; Rietveld, G. Empowering Electric Vehicles Batteries: A Comprehensive Look at the Application and Challenges of Second-Life Batteries. *Batteries* **2024**, *10*, 161. [[CrossRef](#)]

Disclaimer/Publisher’s Note: The statements, opinions and data contained in all publications are solely those of the individual author(s) and contributor(s) and not of MDPI and/or the editor(s). MDPI and/or the editor(s) disclaim responsibility for any injury to people or property resulting from any ideas, methods, instructions or products referred to in the content.